Photophysical Properties of Hemicyanine Dyes Intercalated in Na−Fluorine Mica

Jiho Kim and Minyung Lee*

Department of Chemistry, Ewha Womans University, Seoul 120-750, Korea

Jae-Hun Yang and Jin-Ho Choy

Department of Chemistry, Seoul National University, Seoul 151-742, Korea

Received: August 5, 1999; In Final Form: October 14, 1999

Four dyes (2-DASPI, 4-DASPI, LDS698, and LDS722) derived from the stilbazolium skeleton have been intercalated into optically transparent Na−fluorine mica layers. X-ray diffraction data show that the long axis of DASPI dyes is aligned parallel to the layer, largely maintaining their solution phase structure. On the other hand, conformation of LDS dyes appears to be significantly distorted, due to the two-dimensional confinement. A huge difference in the fluorescence lifetimes between DASPI and LDS dyes in mica was described by the chromophore molecular structures.

Introduction

The photophysics and photochemistry of organic compounds intercalated into layered materials have attracted a lot of recent attention, owing to their potential application in molecular electronics or nonlinear optics.[1−4] The intercalated compounds having two-dimensionally confined molecular structures exhibit many interesting features that do not appear in bulk solution.[5−7] Large molecules like enzymes or DNA as well as organic dyes can be accommodated in layered compounds, because of the large expandability of the interlayer space.[8−10] Among the photophysical properties of intercalated compounds, the most attention has been paid to their steady state absorption, emission, and optical nonlinearities. However, studies on the excited state dynamics of the intercalated molecules in such a two-dimensionally restricted geometry should also be fascinating, as long as their microstructures are well characterized.

This work concerns the molecular structure and, if any, internal twisting dynamics of hemicyanine dyes inserted into the interlayers of Na−fluorine mica. Hemicyanine dyes are positively charged molecules, having an amino group in one end and alkylpyridinium group in the other end. Photophysical properties of the hemicyanines in homogeneous media are well documented.[11−15] As an example, it has been reported that the fluorescence quantum yield of a hemicyanine dye (4-DASPI) is very low in bulk solution, due to the ultrafast twisting process in the excited state.[11,12] The molecules possess several internal twisting modes that facilitate the isomerizational reaction upon photoexcitation. Many theoretical and experimental studies reveal that the torsion of the aniline moiety is most responsible for the ultrafast nonradiative decay processes.[14,15] When the molecules were introduced into various host materials such as amylose, reverse micelle, etc., the fluorescence quantum yields of the molecules were increased dramatically, owing to the slowdown of the internal motion.[16−21] The dyes are also known to possess a high value of the molecular hyperpolarizability ($\beta \approx 10^{-27}$ esu), due to the intramolecular charge transfer character.[22] Unfortunately, the molecular crystal of the dye is centrosymmetric, which makes the bulk second nonlinearity diminish. By employing several processing techniques, non-centrosymmetric molecular assemblies of the dyes have been obtained in LB films and in layered inorganic materials.[3,4,23]

As a host matrix, Na−fluorine mica was chosen in this study because it has been known to possess high crystallinity, controllable composition, and optical transparency in the visible region.[2] The layered material has the capability of accommodating positively charged guest compounds by the ion-exchange method. Hemicyanine dyes chosen as the intercalator were 2-DASPI (2-[4-(dimethylamino)styryl]-1-methylpyridinium iodide), 4-DASPI (*trans*-4-[4-(dimethylamino)styryl]-1-methylpyridinium iodide), LDS698 (1-ethyl-2-(4-(*p*-dimethylaminophenyl)-1,3-butadienyl)pyridinium perchlorate), and LDS722 (1-ethyl-4-(4-(*p*-dimethylaminophenyl)-1,3-butadienyl)pyridinium perchlorate). The molecular structures of four dyes are shown in Figure 1. 2-DASPI and 4-DASPI are isomers with the methylpyridinium group in different positions. LDS698 and LDS722 are also such an isomer, but they have one more double bond with an ethyl substituent at the pyridinium group, instead of the methyl.

The structure of this paper is organized in the following way. The steady state absorption, emission, and fluorescence lifetimes of the dyes are measured in ethanol, and the excited state dynamics of four dyes in solution phase are described. The fluorescence lifetimes of those dyes embedded in PMMA polymer and in powder form are also obtained. The X-ray patterns of the intercalated compounds in mica are analyzed in terms of the molecular structures of the dyes. Finally, the fluorescence lifetime data of the dyes in mica are interpreted, on the basis of the host's microstructure and the guest's molecular structure.

Experimental Section

DASPI dyes were obtained from Aldrich, and LDS dyes were from Exciton. PMMA powders (average molecular weight 120 000) were purchased from Aldrich. Na−fluorine mica ($Na_{0.7}(Mg_{2.65}Si_4)O_{10}F_2$) was obtained from CO−OP Chemicals (Tokyo, Japan). Dye-dispersed PMMA films were prepared by

---

* To whom correspondence should be addressed. Tel: 82-2-3277-2383. Fax: 82-2-3277-2384. E-mail: mylee@mm.ewha.ac.kr.

10.1021/jp9927855 CCC: $19.00

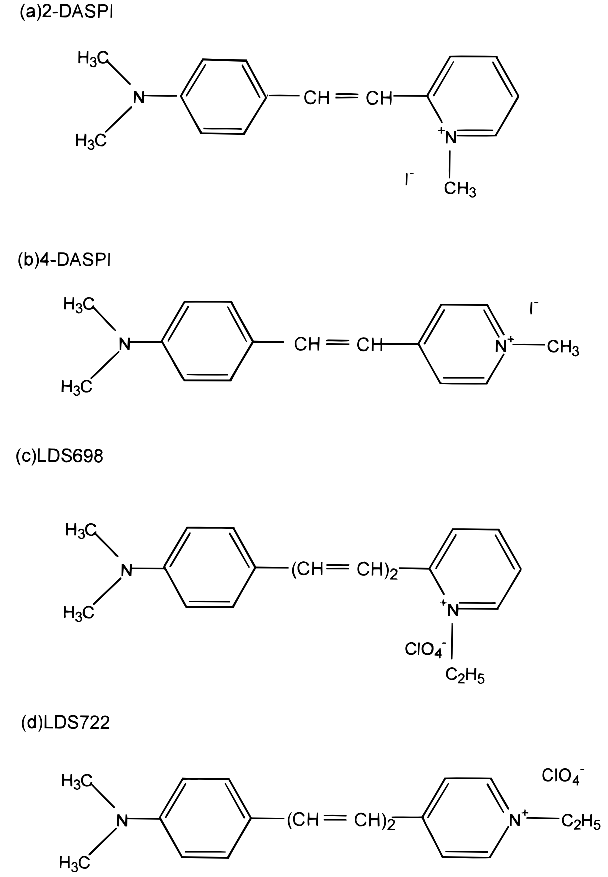

Figure 1. Molecular structures of (a) 2-DASPI, (b) 4-DASPI, (c) LDS698, and (d) LDS722.

spreading monochlorobenzene solutions containing 0.1 g of hemicyanine dyes and 1.0 g of PMMA onto a glass substrate using a spin-coater. The films were dried at 100 °C for a couple of hours to evaporate solvents. The intercalation compounds were prepared by the conventional ion-exchange method. Before the dyes were embedded, mica powder was dried at 600 °C to eliminate water contained in the layer. An aqueous suspension of mica was mixed with an ethanol solution of hemicyanine dyes, and the mixture was allowed to react at 65 °C. The amount of added dyes was 1.5 times of the cation exchange capacity of mica. After the ion exchange, the products were washed with a 50% ethanol solution. This procedure was repeated three times and the product was dried in an oven.

The X-ray powder diffraction (XRD) data of the samples were collected by using a Phillips PW1830 diffractometer equipped with Ni-filtered Cu $K\alpha$ radiation. Diffuse reflectance absorption spectra were obtained by a Shimadzu UV−vis−near-IR scanning spectrophotometer (model UV-3101PC). Emission spectra were recorded by a Photon Technology International fluorescence spectrometer (model 2060A). Fluorescence lifetimes were measured by the time-correlated single photon counting (TCSPC) method, details of which were described elsewhere.[15] Briefly, the sample was excited by the second harmonic (523.5 nm) from a picosecond Nd:YLF laser. The fluorescence was collected by *f*/4 optics and a MCP-PMT (Hamamatsu R3809-07). The instrument response function of the TCSPC system was typically 60 ps. The fluorescence signal was detected at the maximum of the emission spectra. Figure 2 shows the fluorescence decay curves of 4-DASPI in various media. Those of other dyes were also measured in various media and the fluorescence lifetimes were obtained by exponential fitting and from deconvolution analysis.

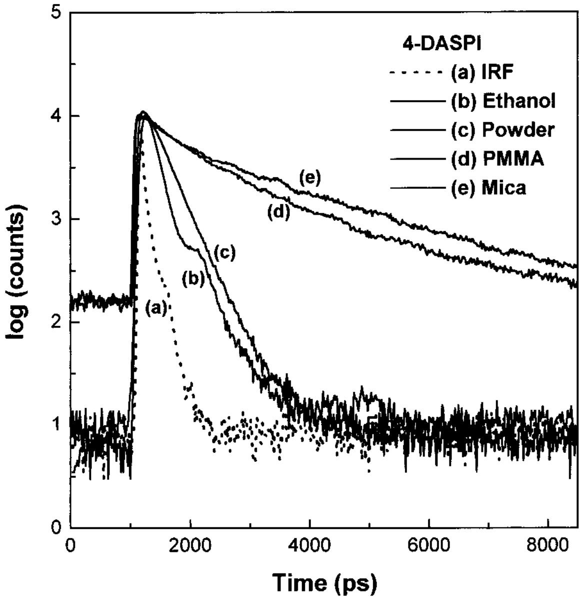

Figure 2. Representative decay curves of 4-DASPI in various media with the instrument response function.

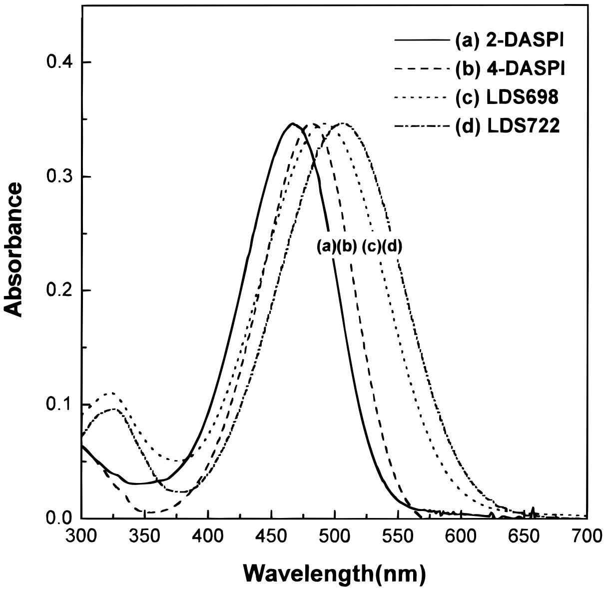

Figure 3. Absorption spectra of hemicyanine dyes in ethanol. 2-DASPI 9.1×10^{-6} M; 4-DASPI 7.1×10^{-6} M; LDS698 9.1×10^{-6} M; LDS722 8.2×10^{-6} M.

Results and Discussion

Photophysics of Hemicyanine Dyes in Solution. In order to understand more fully the photophysical properties of the intercalated compounds, studies in solution phase are necessary as a prerequisite. Figures 3 and 4 show the absorption spectra and emission spectra of hemicyanine dyes in ethanol, respectively. The absorption and emission maxima were shifted to the longer wavelength on the order of 2-DASPI < 4-DASPI < LDS698 < LDS722. Instead of going into details for steady state spectroscopic properties, the fluorescence lifetimes for each dye were measured because they give direct information on the excited state dynamics. Table 1 shows the measured lifetime data of four dyes in ethanol. Although the decay data of all hemicyanine dyes were arbitrarily fit to a double-exponential form, the fluorescence decay of hemicyanine dyes may be nonexponential, as already known for 4-DASPI.[15] In this case, the average lifetime, $\langle \tau \rangle$, is more meaningful, and it is also

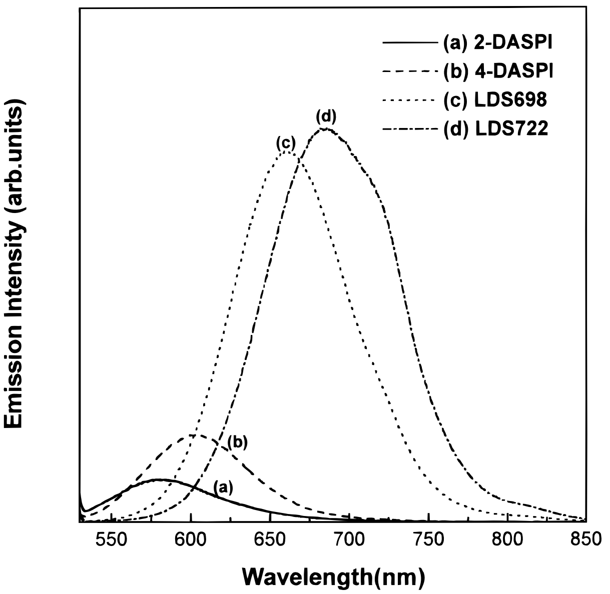

Figure 4. Emission spectra of hemicyanine dyes in ethanol, excited at 523.5 nm. The dye concentrations are the same as those in Figure 3.

TABLE 1: Fluorescence Decay Data of Hemicyanine Dyes in Ethanol, Obtained by the Double-Exponential Fit[a]

	EM[b] (nm)	A_1	τ_1 (ns)	A_2	τ_2 (ns)	$\langle\tau\rangle$[c] (ns)	χ^2
2-DASPI	585	0.68	0.01	0.32	0.06	0.03	2.01
4-DASPI	606	1.00	0.05			0.05	1.90
LDS698	666	0.30	0.06	0.70	0.36	0.27	2.13
LDS722	689	0.22	0.03	0.78	0.54	0.42	1.55

[a] The goodness of the fit is indicated by the value of the reduced χ^2. [b] Emission maximum. [c] $\langle\tau\rangle = A_1\tau_1 + A_2\tau_2$; $A_1 + A_2 = 1$.

shown in the table. The lifetime of 4-DASPI in ethanol, being 50 ps, was about 5 times slower than that in water. The lifetime gets 60% longer when the alkyl substituent at the pyridinium group is located at the 4- rather than at the 2-position. The data also show that the fluorescence lifetimes of LDS dyes having one more double bond than DASPI are about 1 order longer.

The fluorescence lifetimes of DASPI dyes varied from tens to 700−800 ps with changing the solvent from ethanol to cyclohexanol. This results largely from the solvent viscosity change because the viscosity of cyclohexanol is ca. 50 times higher than that of ethanol. For hemicyanine dyes, the major deactivation of the excited state population is caused by forming the TICT state, which is nonfluorescing. The internal twisting motion of the aniline moiety leads to the formation of the TICT state. Therefore, in addition to solvent viscosity, the excited state lifetimes of hemicyanine dyes might be influenced by the solvent polarity that alters the excited state potential surface. For 4-DASPI, the influence of solvent polarity on the excited state potential surface has been thoroughly investigated by McHale and co-workers, employing computer simulation and spectroscopic measurements.[14,24] Their results can be generalized to other hemicyanine dyes, in terms of the fluorescence lifetime data: 2-DASPI seems to behave like 4-DASPI, and LDS dyes have larger activation energy than DASPI for the TICT state formation process.

Excited State Dynamics in PMMA and in Powder. As a series of researches on the internal twisting dynamics of hemicyanine dyes, we have previously studied the excited state dynamics of 4-DASPI in reverse micelle systems.[15] 4-DASPI had the longer lifetime when it was solvated by nanometer-sized water pools formed in AOT reverse micelles. This has been attributed to the slowdown of the internal twisting motion of 4-DASPI in AOT reverse micelles. The rate constant of the internal twisting motion of 4-DASPI increases nonmonotonically with increasing the micelle size. Although it is somewhat flexible, the reverse micellar system provides a three-dimensional confinement for molecules in motion.

TABLE 2: Fluorescence Decay Data of Hemicyanine Dyes in PMMA, Obtained by the Double-Exponential Fit[a]

	EM[b] (nm)	A_1	τ_1 (ns)	A_2	τ_2 (ns)	$\langle\tau\rangle$[c] (ns)	χ^2
2-DASPI	577	0.56	0.30	0.44	1.87	0.99	2.18
4-DASPI	576	0.51	0.26	0.49	2.03	1.12	2.04
LDS698	605	0.43	0.29	0.57	1.73	1.12	1.77
LDS722	615	0.51	0.28	0.48	1.72	0.95	2.05

[a] The goodness of the fit is indicated by the value of the reduced χ^2. [b] Emission maximum. [c] $\langle\tau\rangle = A_1\tau_1 + A_2\tau_2$; $A_1 + A_2 = 1$.

TABLE 3: Fluorescence Decay Data of Hemicyanine Dyes in Powder Form, Obtained by the Double-Exponential Fit[a]

	EM[b] (nm)	A_1	τ_1 (ns)	A_2	τ_2 (ns)	$\langle\tau\rangle$[c] (ns)	χ^2
2-DASPI	651	0.32	0.23	0.68	0.44	0.37	1.55
4-DASPI	667	0.88	0.26	0.12	0.44	0.28	2.66
LDS698	725	0.46	0.37	0.54	1.91	1.20	1.67
LDS722	676	0.49	0.46	0.51	1.46	0.97	1.90

[a] The goodness of the fit is indicated by the value of the reduced χ^2. [b] Emission maximum. [c] $\langle\tau\rangle = A_1\tau_1 + A_2\tau_2$; $A_1 + A_2 = 1$.

We can expect that the large-amplitude motion might be completely blocked when hemicyanine dyes were embedded in a more rigid matrix. In Table 2, the emission maxima of hemicyanine dyes doped in PMMA polymer were shown. Interestingly, they are all blue-shifted from the data in ethanol. This means that PMMA matrix does not allow the photoexcited molecules emit photons in the relaxed state, due to the rigidity of the environment. Table 2 also shows the fluorescence lifetime data of four hemicyanine dyes in PMMA matrix. The average lifetimes for each dye were obtained after fitting to a double-exponential form; they all lie in the couple of nanoseconds range. Since these values approach the radiative lifetimes, there is a strong indication that the conformational change does not occur in the excited state.

The fluorescence lifetimes of four dyes were also measured in powder form. As seen in Table 3, the average lifetimes are longer than those in ethanol, but shorter than those in PMMA. The dye powders may exist as polycrystals or some types of molecular aggregates. In any case, the lifetime data indicate that its environmental rigidity is softer than PMMA polymer. It is interesting that, in contrast to the solution data, the lifetimes of 2-DASPI and LDS698 are longer than those of 4-DASPI and LDS722 in powder form, respectively.

X-ray Data of Dye-Intercalated Mica. X-ray diffraction patterns of pristine and intercalated compounds were measured using the conventional powder method. The diffraction data of the anhydrous mica, not containing dyes, are shown in Figure 5a. The X-ray diffraction pattern of Na−fluorine mica shows the (00*l*) peak, which arises from two tetrahedral SiO_4 sheets between which cations are octahedrally coordinated.[2] In layered compounds, the basal spacing, the distance between two layers, is the most important parameter determining their structures. Using Scherrer's formula, the basal spacing value of 9.6 Å was obtained for the pristine mica. Figure 5 also shows the mica samples intercalated with dye molecules (2-DASPI, 4-DASPI, LDS698, and LDS722). They all exhibit the sharp diffraction peaks, ensuring that the intercalation compounds are homogeneous in structure with good crystallinity. Accommodation of guest molecules into interlayers of mica is accomplished at the expense of the expansion of the basal spacing. The diffraction

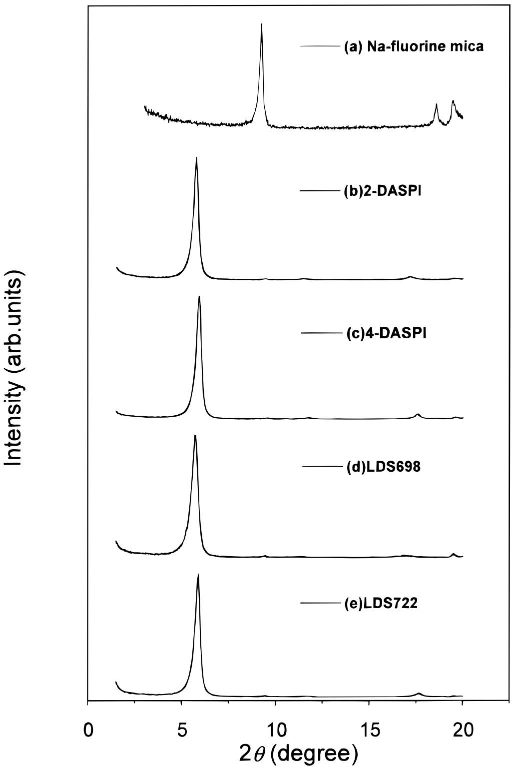

Figure 5. X-ray diffraction patterns of pristine Na−fluorine mica (a) and dye-intercalated mica (b−e).

peaks of the intercalated compounds were significantly shifted from that of the pristine mica. The calculated basal spacing values of 4-DASPI and LDS722 intercalated compounds are the exactly same (15.0 Å), but 2-DASPI and LDS698 have different values, being 15.3 and 15.5 Å, respectively.

The X-ray diffraction studies give information on the orientation of the intercalated species as well as the interlayer distance. The X-ray structure of MPS_3 (M = Cd, Mn) layered compounds intercalated by 4-DASPI has been studied by the Clement group.[3,4] An increase of 6 Å for the basal spacing was observed after intercalation. They suggested that the long axis of molecule is aligned parallel to the layer, but two aromatic rings of DASPI dyes stand nearly perpendicular to the layer. 4-DASPI in mica is expected to have a similar conformation because our obtained value of 5.4 Å is in reasonable agreement with their results. Compared with 4-DASPI, the basal spacing of 2-DASPI-intercalated compounds is 0.3 Å longer. This can be understood considering the substitution position of the methyl group. The schematic diagram for DASPI intercalation compounds are drawn in Figure 6.

It is unusual that the basal spacing of LDS722 is exactly the same as that of 4-DASPI because LDS722 has one more double bond. If all-trans LDS722 dyes maintain the solution phase structure in mica, the length of the short axis of all-trans LDS dyes should be longer by 1.4 Å, compared to DASPI. Since the basal spacing of LDS722 intercalation compounds is similar to that of DASPI, the conformation should be different from the stable equilibrium structure in the solution phase. One interpretation is that LDS722 should be distorted as intercalated into the mica layer. The same notion can be applied to the case of LDS698. The reason why the basal spacing value of LDS698 is 0.5 Å longer than that of LDS722 is that the ethyl substituent is located at the ortho position rather than para.

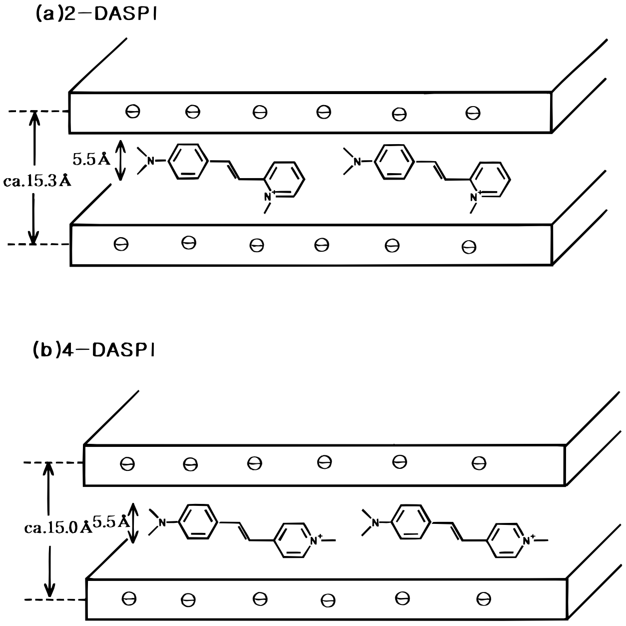

Figure 6. Schematic representation for the alignment of hemicyanie dyes (2-DASPI and 4-DASPI) in the interlayer space of Na−fluorine mica.

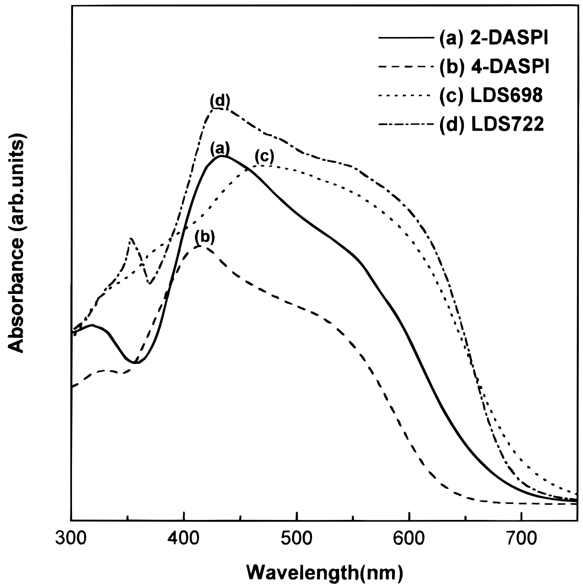

Figure 7. Absorption spectra of hemicyanine dyes intercalated into mica.

Photophysics of Hemicyanine Dyes in Mica. Absorptions of four hemicyanine dyes intercalated in Na−fluorine mica are shown in Figure 7. As known previously, absorption spectra of hemicyanine dyes critically depend on the environment. The four hemicyanine dyes used in this study are all push−pull type molecules, having the electron donor, $-N(CH_3)_2$, on one end, and the electron acceptor, $-NR_2^+$ (R = methyl, ethyl), on the other end. Because of their strong charge transfer character, the absorption spectra are influenced by medium polarity, as seen in the solution phase. When they are intercalated into Na−fluorine mica, deformation of the charge transfer band was observed. The absorption peaks of four dyes are located in the range of 400−450 nm. These peaks are significantly blue-shifted, as compared to ethanol solution data. The peak positions are rather similar to those in aqueous solution. In addition, hemicyanine dyes in mica present a new broad band in 500−650 nm with respect to the bulk solution. In solution, the peaks of the absorption spectra of LDS dyes occur at the longer wavelength, compared with DASPI. The similarity of absorption

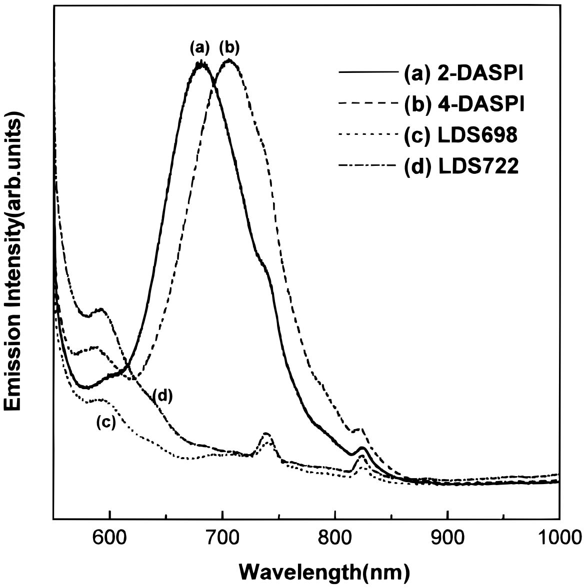

Figure 8. Emission spectra of hemicyanine dyes intercalated into mica.

TABLE 4: Fluorescence Decay Data of Hemicyanine Dyes in Mica, Obtained by the Double-Exponential Fit

	EM^b (nm)	A_1	τ_1 (ns)	A_2	τ_2 (ns)	$\langle\tau\rangle^c$ (ns)	χ^2
2-DASPI	681	0.33	0.33	0.67	2.99	2.11	2.45
4-DASPI	706	0.46	0.45	0.54	1.75	1.15	2.00
LDS698	707	0.79	0.05	0.21	0.20	0.08	1.41
LDS722	727	0.88	0.02	0.12	0.13	0.03	1.57

[a] The goodness of the fit is indicated by the value of the reduced χ^2. [b] Emission maximum. [c] $\langle\tau\rangle = A_1\tau_1 + A_2\tau_2$; $A_1 + A_2 = 1$.

spectra between DASPI and LDS dyes indicates that LDS dyes are distorted in mica, causing the effective π-conjugation to decrease. The broad absorption band occurring at the longer wavelength was previously defined as the metachromacy effect. That is, it may be due to the self-aggregation of dyes or π-electron interaction between of the aromatic dyes and the electron lone pairs of the oxygen atoms of mica surface. As an example, 4-DASPI intercalated into MPS_3 exhibited a strong and broad peak in 580−600 nm. Clement et al. suggested that the guest molecules are packed “edge-on” relative to the host lattice layer, thus facilitating a strong $\pi-\pi$ interaction between chromophores.[4]

Figure 8 shows fluorescence spectra of hemicyanine dyes intercalated into Na−fluorine mica. As is seen in the figure, the fluorescence intensity of 2-DASPI and 4-DASPI restricted in Na−fluorine mica was very strong, resulting from the slowdown of the aniline motion that happens to lead to the TICT state. In contrast, the fluorescence intensity of LDS698 and LDS722 in Na−fluorine mica was very weak. This means that photoexcited LDS dyes deactivate rapidly. Table 4 shows the fluorescence lifetime data of hemicyanine dyes in mica. After intercalation, the lifetimes of both 2-DASPI and 4-DASPI dramatically increase. This is in accordance with the fact that the emission intensity of DASPI increases after intercalation. Comparing the lifetimes of DASPI in Na−fluorine mica with those in ethanol, there is about a 50-fold increase in the fluorescence lifetime. This suggests that the layered structure of Na−fluorine mica provides a restricted environment for DASPI dyes.

LDS dyes also experience two-dimensional confinement in the mica layer, but, unlike DASPI, we see a dramatic decrease in the fluorescence lifetimes of LDS dyes. The average lifetimes of LDS698 and LDS722 are 80 and 30 ps, respectively. The lifetimes are even shorter than those in ethanol. It cannot be explained by aggregate formation because LDS dye powder shows a long (ca. 1 ns) lifetime. In principle, the dye−mica interaction should contribute to the lifetime reduction to some extent, but, as seen in DASPI, it appeared to be negligible. We think that the lifetime shortening arises from the significant distortion of LDS dyes in mica layers. In comparison with DASPI, the geometrical change of LDS dyes in mica has been verified by X-ray diffraction data. Twisting of the aniline moiety cannot occur in mica, owing to the geometrical constraint. Therefore, it is possible that LDS dyes may exist as a cis-like structure that fluoresces weakly, due to a fast nonradiative decay process. However, to explain our observations precisely, further spectroscopic information is necessary. Probably, as already performed by McHale and co-workers in the case of solution phase hemicyanine dyes,[24] a resonance Raman study for the intercalation compounds may identify the molecular structures of the dye molecules in mica.

Conclusion

Picosecond lifetime measurements showed that four hemicyanine dyes (2-DASPI, 4-DASPI, LDS698, and LDS722) in solution undergo fast twisting motion in the excited state. When DASPI dyes were intercalated into Na−fluorine mica, their fluorescence lifetimes were increased, owing to the slowdown of the twisting motion of DASPI dyes in the restricted geometry. In contrast, it was observed that the fluorescence lifetimes of LDS dyes were shortened to a large extent by intercalation. It can be concluded that DASPI dyes in mica maintain their solution phase structures, while conformations of LDS dyes are significantly distorted from the stable forms, as intercalated into the mica layers.

Acknowledgment. This work was financially supported by MOST through the Women’s University Research Fund.

References and Notes

(1) Lacroix, P. G.; Clement, R.; Nakatani, K.; Zyss, J.; Ledoux, I. *Science* **1994**, *263*, 658.
(2) Ogawa, M.; Kuroda, K. *Chem. Rev.* **1995**, *95*, 399.
(3) Coradin, T.; Clement, R.; Lacroix, P. G.; Nakatani, K. *Chem. Mater.* **1996**, *8*, 2153.
(4) Lagadic, I.; Lacroix, P. G.; Clement, R. *Chem. Mater.* **1997**, *9*, 2012.
(5) Villemure, G.; Detellier, C.; Szabo, A. G. *Langmuir* **1991**, *7*, 1215.
(6) Ogawa, M.; Aono, T.; Kuroda, K.; Kato, C. *Langmuir* **1993**, *9*, 1529.
(7) Tamura, K.; Nakazawa, H. *Clay−Clay Mineral.* **1996**, *4*, 501.
(8) Kanzaki, Y.; Hayashi, M.; Minami, C.; Inoue, Y.; Kogure, M.; Watanabe, Y.; Tanaka, T. *Langmuir* **1997**, *13*, 3674.
(9) Choi, J.-H.; Kwak, S.-Y.; Han, Y.-S.; Kim, B.-W. *Mater. Lett.* **1997**, *33*, 143.
(10) Choi, J.-H.; Kwak, S.-Y.; Park, J.-S.; Jeong, Y.-J.; Portier, J. *J. Am. Chem. Soc.* **1999**, *121*, 1399.
(11) Gorner, H.; Gruen, H. *J. Photochem.* **1985**, *28*, 329.
(12) Fromherz, P.; Heilemann, A. *J. Phys. Chem.* **1992**, *96*, 6864.
(13) Strehmel, B.; Seifert, H.; Rettig, W. *J. Phys. Chem.* **1997**, *101*, 2232.
(14) Cao, X.; Tolbert, R. W.; McHale, J. L.; Edwards, W. D. *J. Phys. Chem. A* **1998**, *102*, 2739.
(15) Kim, J.; Lee, M. *J. Phys. Chem. A* **1999**, *103*, 3378.
(16) Hall, R. A.; Thistlethwaite, P. J.; Grieser, F.; Kimizuka, N.; Kunitake, T. *J. Phys. Chem.* **1993**, *97*, 11974.
(17) Fromherz, P. *J. Phys. Chem.* **1995**, *99*, 7188.
(18) Xu, Z.; Lu, W.; Bohn, P. *J. Phys. Chem.* **1995**, *99*, 7154.
(19) Kim, O.-K.; Choi, L.-S.; Zhang, H.-Y.; He, X.-H.; Shih, Y.-H. *J. Am. Chem.* Soc. **1996**, *118*, 12220.
(20) Ogawa, M. *Chem. Mater.* **1996**, *8*, 1347.
(21) Lang, A.-D.; Zhai, J.; Huang, C.-H.; Gan, L.-B.; Zhao, Y.-L.; Zhou, D.-J.; Chen, Z.-D. *J. Phys. Chem.* **1998**, *102*, 1424.
(22) Narang, U.; Zhao, C. F.; Bhawalkar, J. D.; Bright, F. V.; Prasad, P. N. *J. Phys. Chem.* **1996**, *100*, 4521.
(23) Xu, J.; Han, K.; Zhou, G.; Zhang, Z. *Langmuir* **1997**, *13*, 3187.
(24) Cao, X.; McHale, J. L. *J. Chem. Phys.* **1998**, *109*, 1901.